Santa Clara University

Scholar Commons

Electrical and Computer Engineering   School of Engineering

7-16-2022

Stochastic Distributed Control for Arbitrarily Connected Microgrid Clusters

Maryam Khanbaghi
Santa Clara University, mkhanbaghi@scu.edu

Aleksandar Zečević
Santa Clara University, azecevic@scu.edu

Follow this and additional works at: https://scholarcommons.scu.edu/elec

Part of the Electrical and Computer Engineering Commons

Recommended Citation

Stochastic Distributed Control for Arbitrarily Connected Microgrid Clusters

Maryam Khanbaghi *[ORCID] and **Aleksandar Zecevic**

Department of Electrical and Computer Engineering, Santa Clara University, Santa Clara, CA 95053, USA; azecevic@scu.edu
* Correspondence: mkhanbaghi@scu.edu

Abstract: Due to the success of single microgrids, the coming years are likely to see a transformation of the current electric power system to a multiple microgrid network. Despite its obvious promise, however, this paradigm still faces many challenges, particularly when it comes to the control and coordination of energy exchanges between subsystems. In view of that, in this paper we propose an optimal stochastic control strategy in which microgrids are modeled as stochastic hybrid dynamic systems. The optimal control is based on the jump linear theory and is used as a means to maximize energy storage and the utilization of renewable energy sources in islanded microgrid clusters. Once the gain matrices are obtained, the concept of ε-suboptimality is applied to determine appropriate levels of power exchange between microgrids for any given interconnection pattern. It is shown that this approach can be efficiently applied to large-scale systems and guarantees their connective stability. Simulation results for a three microgrid cluster are provided as proof of concept.

Keywords: microgrid clusters; stochastic control; distributed control; jump linear theory; large-scale systems; energy management

1. Introduction

Microgrids are evolving to become fundamental building blocks in a smart grid, and their proliferation has incentivized utilities to revisit the existing grid management paradigm. Since microgrids (MGs) are controllable entities consisting of interconnected loads and distributed energy resources (DERs), effective energy transfer and coordination between them could help maintain the stability and reliability of regional large-scale power grids. For this reason, in the past two decades a considerable amount of research has been devoted to the design and management of MGs. The IEEE Power and Energy Society task force on MG control has provided a comprehensive review of recent results in this field (see [1] and the references therein).

Connecting multiple MGs can provide additional operational flexibility for large-scale power grids, since it allows them to realize the benefits of variable DERs more effectively. In order to accomplish that, MGs within a region must cooperate with each other in a way that improves efficiency, reliability, and resilience. This means (among other things) that interconnected microgrids should not limit their exchanges to energy generated by renewable sources and should also share energy that is accumulated in their storage devices. Such an approach can improve the local supply and demand balance for each individual microgrid, resulting in a more reliable power supply for consumers. This objective has become increasingly important in light of recent natural disasters in the USA, which have underscored the need to prioritize resiliency over operation costs.

Basic control architectures for multiple microgrids can be categorized as centralized, decentralized, distributed, and hierarchical [2]. This work will focus on distributed control where *both* local measurements *and* information from neighboring units are utilized. The main challenge in this case is how to achieve optimal coordination among the subsystems.

This problem has attracted considerable attention in recent years, and a large body of research has been devoted to the potential benefits that can arise from the coordinated operation management of neighboring microgrids [3]. The solutions that have been proposed so far take many different forms and depend on the types of MGs that are involved, their sizes, and their proximity. A group of MGs that are geographically close and are physically interconnected via dc (or ac) buses is referred to as a *microgrid cluster* [4]. Such clusters typically allow for the maximal utilization of energy sources and can improve reliability. There is a growing interest in such microgrids, due in a large part to the increasing number of dc sources and loads.

Multilevel control schemes are widely accepted as a standard solution for the efficient energy management of multiple MGs. The first of these levels (which is known as primary control) is responsible for regulating local voltage and frequency. It normally follows the set-points provided by higher level controllers and performs control actions over interface power converters. Secondary control deals with system-level issues, such as power quality regulation, the synchronization of MGs with the external network, the coordination of distributed generation, and so on. Tertiary control is tasked with optimization, management, and overall system regulation. It should be noted in this context that primary and secondary control levels are associated with the operation of individual MGs, while tertiary control pertains to the coordinated operation between MGs and the utility grid [1].

Most existing papers on distributed tertiary control focus on enhanced efficiency and balanced power flow between the MG and the utility grid, taking into account optimality, stability, and economic factors. The distributed power management between MGs within a cluster has also been studied (see, for example, [5–11] and the references therein). It is interesting to note, however, that only a handful of papers have examined MG clusters as a possible way to cope with the intermittence and randomness of renewable energy [12–19]. Some of the most recent work on this subject considers a hierarchical control scheme and a corresponding consensus-based multilayered event-triggered control algorithm for MG clusters [20]. There have also been some new results related to distributed optimization at the MG cluster level [21], and the problem of distribution load sharing [22].

Although these references offer a variety of different approaches, there is a general agreement that stability and reliability can be greatly improved by connecting MGs directly to the utility grid, or by forming clusters of interconnected MGs [23]. In view of that, in this paper we propose a distributed control strategy for MG clusters that operate in the islanded mode. What makes this strategy unique is the fact that it simultaneously addresses two different types of uncertainties in the system: the inherent randomness of renewable generation (such as solar energy), and unpredictable changes in the system topology that can arise as a result of natural disasters and/or extreme operating conditions. The main advantages of this approach can be summarized as follows:

(1) The dynamic model that is proposed is linear and hybrid. It incorporates the stochastic nature of renewable sources and can accommodate arbitrary energy exchange patterns between the MGs. Such a model is required in order to analytically determine the control gains, and its simplicity ensures that the necessary computations can be performed efficiently.

(2) An optimal control strategy is developed to maximize the energy storage of each MG. This is accomplished by regulating the power flow between MGs using a modified version of the so-called ε-suboptimality theorem [24], which is suitable for large-scale systems. This result allows for arbitrary interconnection patterns between MGs and guarantees a desired level of suboptimality in all cases.

(3) The control law (which is based on the jump linear theory [25]) is designed to ensure stability under structural perturbations, while minimizing the error between the load demand (set point) and generation.

(4) The gain matrix can be calculated offline for all relevant generation patterns. We can do so analytically using the proposed dynamic model, and the necessary computations can be performed in a multiprocessor environment (since each gain matrix is

determined independently). Something similar can be said for computations related to ε-suboptimality, which can be performed efficiently even when the system is large (due to the special structure of the dynamic model).

The paper is organized as follows. In Section 2, we present a simplified model for flexible MG clusters that takes into account power exchanges between MGs. We then proceed to develop a stochastic optimal control strategy, which is described in Section 3. In Section 4, we explain how the ε-suboptimality theorem can be used to achieve maximal power transfer between MGs. Simulation results and their analysis are provided in Section 5. Since the example that we consider serves primarily as a proof of concept, we focused on clusters that contain less than five MGs and have a peak load of less than 10 MW. This assumption is not necessary from a theoretical standpoint, but it has some practical benefits when it comes to simulation. We conclude with a discussion of the potential advantages of this approach and a brief overview of future directions for future research.

2. System Description and Mathematical Modeling

We begin this section by offering a general system description for multiple interconnected MGs. We will then introduce a simple mathematical model that represents an extension of the one proposed in [26]. This model will be utilized to develop a stochastic multivariate optimal control strategy, whose objective is to address some recent challenges in the energy management of multiple MGs. As noted in the Introduction, we will focus on interconnected MGs that are disconnected from the utility grid and are geographically close to each other.

2.1. System Description

Figure 1 provides a schematic representation of multiple MGs that can exchange energy with each other in an arbitrary manner. Although the microgrids in this diagram are disconnected from the utility grid, we should point out that the connection can be reestablished whenever that becomes necessary. The MGs are concentrated in a relatively small geographic area and are connected to a common bus through a static switch. In configurations of this sort (which are known as clustered MGs), it is assumed that each subsystem can share its energy needs via a communication network. This assumption is realistic in a smart grid since smart meters are capable of broadcasting data over a network.
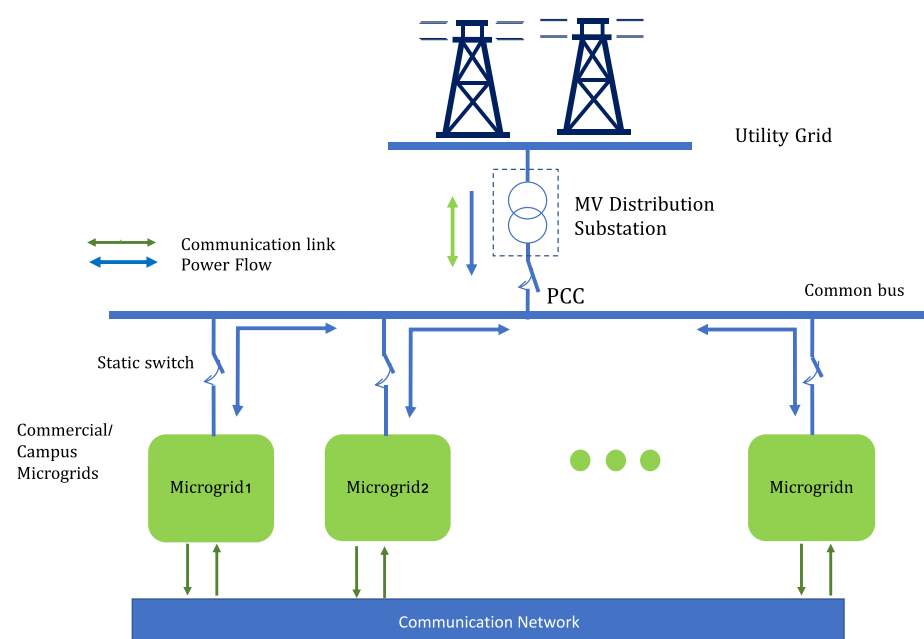
Figure 1. Schematic of multiple MGs that are connected to a common bus by static switches and can exchange information via a communication network.

Throughout this study, we will distinguish between two modes of operation—The *interconnected* mode (in which multiple MGs can exchange energy) and the *disconnected* mode, in which this is not possible. The latter configuration (and the one where MGs are connected to the utility grid) was considered in our previous work [26] and will be used here only for comparison purposes. Our objective in this paper will be to achieve optimal energy management of interconnected multiple MGs by maximizing the battery storage capacity usage, as well as the utilization of solar energy.

Since the focus of our work is distributed tertiary control in a hierarchical architecture, a continuous dynamic model for structures of this type will be proposed in the next section. We will concentrate primarily on commercial MGs (including university campuses), since systems of this sort have two important features that allow us to develop an effective and robust control strategy:

- Although each MG load can be comprised of multiple buildings (with varying energy demands), its aggregated power has a predictable profile.
- The load demand reaches its peak during the day (when solar energy is typically available) and becomes minimal at the end of the day as residential loads start peaking.

In modeling the dynamic behavior of MGs, we will assume that each MG can be connected to or disconnected from the cluster in a random manner, depending on its load, its generation needs, and its ability to share energy. In the proposed model, individual MGs are controlled using locally available information, while energy exchanges are based on global information. The control law must ensure that stability (and an acceptable level of suboptimality) is retained for *all* possible interconnection patterns. Closed loop systems that have this property are said to be *connectively stable* [24].

In the model that we will be working with, each MG consists of a specific load (commercial or a university campus), battery storage, and an array of solar cells. When it is in the *disconnected mode*, solar energy is provided internally, and is distributed to the battery and the load in a way that reflects the load requirements. During the night, it is assumed that the battery is the sole source of energy. This is a reasonable assumption, since most large commercial consumers require less energy during the night than during the day. In situations where the required battery storage is not available, a secondary dispatchable generation source (such as a fuel cell, for example) may be considered. We should point out, however, that such additions have little effect on our control strategy, so we will disregard them in our analysis. When MGs operate in the *interconnected mode*, each of them can deliver power to other MGs provided that their own load requirements are satisfied. The shared energy can then be used to charge the batteries of microgrids whose storage levels are not sufficiently high.

2.1.1. The Load Model

In the simplified scenario that we just described, the primary goal is to manage the energy demand in a system that consists of n microgrids. This is done by balancing the real power generated by the PV array ($P_{solar}^{(m)}$) and the battery ($P_B^{dis(m)}$) in MG m with the power required by the load ($P_L^{(m)}$), and the power that MG m exchanges with other MGs (which will be denoted in the following by $P_{ex}^{(m)}$). Note that $P_{ex}^{(m)}$ will be positive if MG m delivers energy to the network, and negative if this microgrid absorbs energy. Using this notation, we can express the power balance as:

$$P_L^{(m)}(t) = \alpha_m P_{solar}^{(m)}(t) + P_B^{dis(m)}(t) - P_{ex}^{(m)}(t) \tag{1}$$

where parameter α_m represents the fraction of solar power that is delivered to the load (the value of this constant is chosen based on the solar panel size and battery storage capacity). As we already mentioned, it is assumed that $P_L^{(m)}(t)$ follows a known deterministic trajectory, and the power generated by the PV array, $P_{solar}^{(m)}(t)$ will be treated as a random variable whose characteristics depend on cloud coverage and the time of day. Since the

battery can inject power into the system (as well as absorb it when needed), we will treat $P_B^{dis(m)}(t)$ as a control input.

Power losses that are primarily due to transmission lines are neglected in this model, since MGs that belong to the same cluster are considered to be close to each other (by definition). The PV array should be sized in a way that is proportional to the daytime peak load requirements (which is becoming increasingly feasible due to the decreasing cost of solar panels). This ensures full load satisfaction when the weather is sunny. The battery should also be properly sized so that it can meet the night load. Because the excess energy produced by the array can be used to charge the battery, the battery can act as a buffer. This allows the system to use the stored solar energy when the PV array is inactive.

In addition to the relationship described in (1), our model incorporates the following four assumptions:

- Information about the system state (which includes instantaneous power flows, maximal and minimal generation levels, and maximal and minimal battery levels) is readily available. This can be ensured by using a battery state of charge (SoC) tracker, combined with voltage, current, or phasor monitoring devices.
- Only active power is considered, and it is assumed that the controllers/inverters on the PV array and battery regulate voltages and phase angles.
- The data used to represent the commercial load for each MG corresponds to the typical commercial load in the US. This data are provided by National Renewable Energy Laboratory (NREL) and is available online [27].
- Changes in solar generation states are detected via solar radiation sensors.

2.1.2. The Solar Generation Model

Although solar power is a highly desirable form of generation, it has certain intrinsic shortcomings that stem from its intermittent nature. To model the stochastic character of solar generation, a continuous Markov chain will be used to represent different levels of cloud coverage. The details of this model are discussed in [26], so we will only highlight its most pertinent features.

In general, cloud coverage classification should be based on regional weather patterns. This means that the number of relevant scenarios can vary significantly, depending on where the MG cluster is located. The model that we propose allows for this type of flexibility, but in our simulations we will concentrate on a somewhat simpler case, which reflects the weather patterns in northern California. According to the data obtained from the San Jose International Airport meteorological report [28], in northern California it suffices to consider only three different levels of cloud cover: sunny, partly cloudy, and overcast.

At night there is obviously no generation, so the power produced by the PV array, $P_{solar}(t)$, can be represented as a piecewise constant function (where $P_{solar}(t) = 0$ at night and $P_{solar}(t) = P_{solar}(r(t))$ during the day). The term $r(t)$ denotes the state of the Markov chain that corresponds to the cloud coverage during the day. This means that $r(t)$ evolves according to a continuous time Markov chain [22,28], taking values from set $S = \{1, 2, 3\}$ in the geographic region that we are concerned with.

Matrix $P = \{p_{ij}\}$, which characterizes this process, provides the probabilities of transitioning from one state to another, and its elements are given by:

$$p_{ij} = Prob(r(t + \Delta) = j | r(t) = i) \quad \begin{aligned} &= \pi_{ij}\Delta + o(\Delta) &&\text{if } i \neq j \\ &= 1 + \pi_{ii}\Delta + o(\Delta) &&\text{if } i = j \end{aligned} \tag{2}$$

where $\Delta > 0$ and $\lim_{\Delta \to 0} \frac{0(\Delta)}{\Delta} = 0$. In this expression, coefficients π_{ij} represent the (non-negative) transition rate from i to j ($i \neq j$), and π_i is defined as

$$\pi_i \triangleq -\pi_{ii} \triangleq \sum_{j=1,\ j \neq i}^{3} \pi_{ij} \tag{3}$$

Given this notation, the transition rate matrix Π will have the form $\Pi = \{\pi_{ij}\}$ $(i, j = 1, 2, 3)$ [25].

The transition probability matrix and the transition rates that were used in our simulations were calculated from the data set provided in [28] (which contains information gathered between 2008 and 2017). An analysis of this data indicates that the transition probabilities do not change significantly from year to year. As a result, we can assume that the corresponding matrix is fixed for microgrids located in northern California.

2.1.3. The Battery Model

Each microgrid is assumed to have a battery storage system that supplements the intermittent generation from the PV array. Relevant battery characteristics include its energy capacity (more specifically SoC), its charge/discharge powers, its life cycle, as well as its safe operating temperatures. In the following, we will assume that the energy stored in the battery, $E_B(t)$, and the charge/discharge power $P_B(t)$ can be used to provide adequate information about the SoC.

The battery is assumed to have energy limits, $E_{Bmin} \leq E_B(t) \leq E_{Bmax}$, and variations in the stored energy can be described as [29]

$$\frac{dE_B(t)}{dt} = P_B^{ch.}(t) - P_B^{dis.}(t) - \gamma E_B(t) \tag{4}$$

In this expression, $P_B^{ch.} = (1 - \alpha_m)P_{solar}(t)$, γ denotes the rate of self-discharge, and $P_B^{dis.}$ is the battery discharge. We will assume that batteries have the same efficiency when charging and discharging, and that they can easily switch from one mode to the other (this feature becomes important in cases when MGs exchange energy directly). For normal battery operation, it is common to set its upper and lower energy limits to 10% and 90% of the maximum energy that can be stored. By doing so, we can increase the lifespan of the battery.

2.2. Mathematical Modeling

Combining Equations (1) and (4), the energy management of MG m in a system made up of n MGs can be described as:

$$\frac{dE_B^{(m)}}{dt}(t) = (1 - \alpha_m)P_{solar}^{(m)}(t) - P_B^{dis(m)}(t) - \gamma_m E_B^{(m)}(t)$$
$$P_L^{(m)}(t) = \alpha_m P_{solar}^{(m)}(t) + P_B^{dis(m)}(t) - P_{ex}^{(m)}(t) \tag{5}$$

In this expression it is implicitly assumed that there are no energy exchanges with the utility grid since we are interested only in the islanded mode of operation. If MG m has unused energy that it can share, we can represent $P_{ex}^{(m)}(t)$ as $P_{ex}^{(m)}(t) = \frac{dE_{ex}^{(m)}(t)}{dt}$, where $E_{ex}^{(m)}(t)$ is the amount of energy that MG m has delivered to other MGs during the interval $[t_0, t]$ (t_0 being the time when the exchange begins). Since we have the freedom to decide how the energy exchanges are scheduled, we will assume that this is done in such a way that $\frac{dE_{ex}^{(m)}}{dt}$ is proportional to the amount of energy consumed by the load m up to time t. That allows us to express $P_{ex}^{(m)}(t)$ as

$$P_{ex}^{(m)}(t) = \frac{dE_{ex}^{(m)}(t)}{dt} = \sum_{k \neq m} a_{km} E_L^{(m)}(t) \tag{6}$$

where a_{km} determines the fraction of $E_L^{(m)}(t)$ that is transferred from MG m to MG k (note that these coefficients have the appropriate units). Since coefficients a_{km} are adjusted based on the varying energy needs of each microgrid, we will treat their values as uncertain quantities. In the sections that follow, we will explain the constraints that these values must satisfy in order to ensure a desired level of suboptimality.

When microgrid *m delivers* power to other MGs, $P_{ex}^{(m)}$ will have the form shown in Equation (6). Setting

$$a_m = \sum_{k \neq m} a_{km} \tag{7}$$

and recalling that $P_L^{(m)}(t) = \frac{dE_L^{(m)}(t)}{dt}$, Equation (1) becomes

$$\frac{dE_L^{(m)}(t)}{dt} = \alpha_m P_{solar}^{(m)}(t) + P_B^{dis(m)}(t) - a_m E_L^{(m)}(t) \tag{8}$$

In cases when MG *m receives* power from other MGs, $P_{ex}^{(m)}(t)$ is negative, and can be expressed as

$$P_{ex}^{(m)}(t) = \frac{dE_{ex}^{(m)}(t)}{dt} = -\sum_{k \neq m} a_{mk} E_L^{(k)}(t) \tag{9}$$

Under such circumstances, Equation (1) takes the form

$$\frac{dE_L^{(m)}(t)}{dt} = \alpha_m P_{solar}^{(m)}(t) + P_B^{dis(m)}(t) + \sum_{k \neq m} a_{mk} E_L^{(k)}(t) \tag{10}$$

Since a microgrid can either deliver or receive energy, Equations (8) and (10) represent the only possible scenarios for a given MG. This includes situations where certain MGs are disconnected (since we can treat them as a special case of (10) where $a_{mk} = 0$ for all *k*).

One of the principal advantages of the proposed model is that the system can be stabilized using decentralized control *regardless of how coefficients a_{km} are chosen*. In order to demonstrate that, suppose that *q* MGs are absorbing power at some point in time, and that *n − q* are delivering. We can always number the MGs in such a way that the ones that absorb power come *first*. For any such MG, we have that $m \leq q$, and the power balance equation has the form

$$\frac{dE_L^{(m)}(t)}{dt} = \alpha_m P_{solar}^{(m)}(t) + P_B^{dis(m)}(t) + \sum_{k=q+1}^{n} a_{mk} E_L^{(k)}(t) \tag{11}$$

For MGs that deliver power, we have that $m > q$ and

$$\frac{dE_L^{(m)}(t)}{dt} = P_{solar}^{(m)}(t) + P_B^{dis(m)}(t) - a_m E_L^{(m)}(t) \tag{12}$$

Introducing matrices

$$A_{mm} = \begin{pmatrix} -\gamma_m & 0 \\ 0 & -a_m \end{pmatrix}; \quad A_{mk} = \begin{pmatrix} 0 & 0 \\ 0 & a_{mk} \end{pmatrix} \tag{13}$$

and defining vector $P^{(m)} \equiv \left[(1 - \alpha_m) P_{solar}^{(m)} \quad \alpha_m P_{solar}^{(m)} \right]^T$, the *n* subsystems can be represented as

$$\dot{x}_m(t) = A_{mm} x_m(t) + \sum_{k=q+1}^{n} A_{mk} x_k(t) + B_m u_m(t) + P^{(m)} \tag{14}$$

for *m* = 1, 2, $\cdots$, *q*, and

$$\dot{x}_m(t) = A_{mm} x_m(t) + B_m u_m(t) + P^{(m)} \tag{15}$$

for $m = q + 1, \cdots, n$. The overall interconnected system can then be described as

$$\dot{x}(t) = Ax(t) + Bu(t) + P(t) \tag{16}$$

where matrix A has an upper block triangular structure

$$A = \begin{pmatrix} A_{11} & 0 & \cdots & 0 & A_{1,q+1} & \cdots & A_{1n} \\ 0 & A_{22} & \cdots & 0 & A_{2,q+1} & \cdots & A_{2n} \\ \vdots & \vdots & \ddots & \vdots & \vdots & \vdots & \vdots \\ 0 & 0 & \cdots & A_{qq} & A_{q,q+1} & \cdots & A_{qn} \\ 0 & 0 & & 0 & A_{q+1,q+1} & & 0 \\ \vdots & \vdots & \cdots & \vdots & \vdots & \ddots & \vdots \\ 0 & 0 & & 0 & 0 & & A_{nn} \end{pmatrix} \tag{17}$$

and

$$B = diag\ \{\ B_m\ \}, \quad B_m = \begin{bmatrix} -1 & 1 \end{bmatrix}^T \quad m = 1, \ldots, n$$

$$P(t) = \begin{bmatrix} P^{(1)}(t) & \cdots & P^{(n)}(t) \end{bmatrix}^T, \quad x = \begin{bmatrix} x_1 & x_2 \cdots x_n \end{bmatrix}^T = [E_B^{(1)} \ E_L^{(1)} \cdots \ E_B^{(n)} E_L^{(n)}]^T$$

$$u = \begin{bmatrix} u_1 & u_2 \cdots u_n \end{bmatrix}^T = [P_B^{dis(1)} \ P_B^{dis(2)} \cdots \ P_B^{dis(n)}]^T$$

In this system of equations, x denotes the state vector, u represents the control action (which is implemented by charging and discharging batteries), and vector $P(t)$ is the power delivered by the solar panels (a part of which goes to batteries).

The fact that matrix A is upper block triangular is of crucial importance here, because it ensures that the stability of the individual subsystems implies the stability of the overall system. Note that this will be the case regardless of how the microgrids are actually numbered—for stability purposes, it suffices to recognize that a permutation that produces the structure in (17) *exists* for every possible energy exchange pattern. A more general scenario where existence is not guaranteed is described in [30]. In this case, it is necessary to use an efficient decomposition algorithm that can determine an appropriate decentralized control law.

In the worst-case scenario (from a stability perspective), block A_{mm} will have the form

$$A_{mm} = \begin{pmatrix} -\gamma_m & 0 \\ 0 & 0 \end{pmatrix} \tag{18}$$

(blocks of this sort correspond to MGs that are receiving energy). We can easily stabilize any such subsystem ahead of time using decentralized control. As a result, we can ensure that the overall system will be stable for *any* set of coefficients a_{mk} that we choose.

2.3. Microgrid Exchange Protocol

In addition to ensuring stability for arbitrary energy exchange patterns, it is also necessary to develop a systematic procedure that all such exchanges must follow. With that in mind, we propose the following simple scheme:

(a) Each MG that *delivers* energy sends an amount equal to $E_m^+ = a_m E_L^{(m)}$ to the common bus (see Figure 1).
(b) Each MG that *absorbs* energy takes

$$E_m^- = \sum_{k \neq m} a_{mk} E_L^{(k)} \tag{19}$$

from the common bus.

If we adopt this approach, the energy that an individual MG sends through the common bus can be aggregated (which is convenient from a practical perspective). Note, however, that its contribution is uniquely defined by the value of coefficient a_m. The same can be said for the energy absorbed by an MG that requested additional resources, which is determined by coefficients a_{mk}. As a result, the proposed strategy can be easily implemented.

3. Stochastic Control Strategy for Interconnected MGs

Since the system matrix A is always permutable into an upper block triangular form, we have the flexibility to consider a range of possible decentralized control strategies. Given the random nature of solar generation, it would be logical to incorporate stochastic elements into the process for determining the gain matrices. We propose to do so by representing solar generation as a continuous Markov chain and applying jump linear quadratic control to each microgrid (following the ideas introduced in [26,31,32]).

Our principal design objective will be to produce a different gain matrix for each level of cloud coverage and ensure that the load demand is satisfied in all cases. Because each of these scenarios is independent (and can be handled offline), the computation of the gain matrices can be distributed across multiple processors. This obviously contributes to the computational efficiency of the procedure and makes the design safer with respect to potential cyber-attacks (since each subsystem can compute its own gain matrices locally).

In order to describe the proposed control design, we will first provide a brief overview of jump linear systems and optimization techniques that are suitable for them. We will then apply this methodology to interconnected microgrids, where the cost function is defined in terms of deviations from the load demand.

3.1. An Overview of Jump Linear Systems Tracking Problem

The state–space representation of a jump linear system (JLS) for a tracking problem has the general form

$$\dot{\overline{x}}(t) = A(r(t))\overline{x}(t) + B(r(t))u(t); \quad x(t_o) = x_o \tag{20}$$

with $\overline{x}(t) = x(t) - x_0(r(t))$, where $A(r(t))$ and $B(r(t))$ are $n \times n$ and $n \times m$ matrices, respectively, and $r(t)$ denotes the current system mode (which is determined by a finite state Markov jump process). To simplify the notation, in the following we will refer to matrices $[A(r(t)), B(r(t))]|_{r(t)=i}$ as $[A^i, B^i]$ and $x_0(r(t))|_{r(t)=i}$ as x_0^i when the system operates in the ith mode [25]. Since $r(t)$ reflects the cloud coverage during the day, this variable evolves according to a continuous time Markov chain. When designing an optimal controller for such a system, one aims to minimize the quadratic cost function:

$$J(u, t_0, r(t_0), x_0) = E\left\{\int_{t_0}^{t_f} \left(\overline{x}^T(t)Q(r(t))\overline{x}(t) + u^T(t)R(r(t))u(t)\right)dt \mid t_0, r(t_0), x_0\right\} \tag{21}$$

where t_0 and t_f denote the initial and final time, respectively, and E{.} represents the expected value of a random function [25]. The symmetric weighting matrices, $Q(r(t))$ and $R(r(t))$, are mode dependent and are used to tune the system response to fit desired characteristics. In the following, they will be denoted as $[Q^i, R^i]$ with $Q^i \geq 0$ (positive semi-definite) and $R^i > 0$ (positive definite) when the system is operating in its ith mode.

In this paper, we will be primarily interested in the ergodic infinite horizon problem and the steady state values of the control gain. The cost function

$$J = \overline{\lim_{t_f \to \infty}} \frac{1}{t_f} E\left\{\int_{t_0}^{t_f} \overline{x}^T(t)Q^i\overline{x}(t) + u^T(t)R^iu(t))dt\right\} \tag{22}$$

is minimized using the stochastic maximum principle, which produces a time-varying feedback control law affine in state of the form:

$$u^*(t) = -(R^i)^{-1} B^T K_\infty^{\ i} \left(\overline{x}(t) + \eta^i(t) \right) \quad \text{for} \quad r(t) = i \tag{23}$$

where matrices K_∞^i ($i = 1, 2, 3$) satisfy the set of coupled algebraic Riccati equations

$$\left(A^i \right)^T K_\infty^{\ i} + K_\infty^{\ i} A^i + Q^i - K_\infty^{\ i} S^i K_\infty^{\ i} + \sum_{j=1}^{N} \pi_{ij} K_\infty^{\ j} = 0 \tag{24}$$

with $S^i = B^i (R^i)^{-1} (B^i)^T$.

Under stochastic controllability and observability conditions [32], the Riccati gains for the infinite horizon problem will converge to the unique positive definite solutions of the coupled algebraic Riccati equations. Equations of this sort can be solved using the numerical algorithm proposed in [33]. The bias vector $\eta_i(t)$ in (23) satisfies $\eta_i \left(t_f \right) = 0$ ($i = 1, 2, 3$), and evolves according to equation

$$\dot{\eta}^i(t) = \left(A^i + (K^i)^{-1} Q^i \right) \eta^i(t) + \sum_{j=1}^{3} \pi_{ij} (K^i)^{-1} K^j \left(\eta^i(t) - \eta^j(t) - s_{ij} \right) \tag{25}$$

The term s_{ij} should be interpreted as the change in the operating points due to the fact that system transitions from mode i to mode j [31,34]. In this particular case, it is equal to $x_0^i - x_0^j + (A^i)^{-1} \overline{P}^j - (A^i)^{-1} \overline{P}^i$. In the steady state, $\eta^i(t)$ can be easily computed by solving three equations in three unknowns once (24) is solved.

3.2. JLQC Strategy for Interconnected Microgrids

Before we apply this approach to interconnected microgrids, we should first recall that energy exchanges between them are dictated by the needs of each individual MG. Since these needs can vary unpredictably for a given state of cloud coverage, coefficients a_{mk}^i cannot be known in advance. With that in mind, we will perform the optimization on individual microgrids when they are *disconnected* from each other (in which case $a_{mk}^i = 0$ for all m and k).

If we treat the solar energy production of microgrid m as a continuous Markov chain, the power delivered will be a piecewise constant, with the changes coinciding with jumps (it is assumed that these changes can be easily detected via solar radiation sensors). Under such circumstances, microgrid m can be viewed as a continuous linear time invariant system with Markovian jumps and a hybrid (continuous–discrete) state space $[x_m \ i]^T$. The corresponding state space model will have the general form

$$\dot{x}_m(t) = A_{mm}^i x_m(t) + B_m u_m(t) + P_m^i \tag{26}$$

where matrix A_{mm}^i differs from one state of solar energy to another. Note that matrices A_{mk}^i do not appear in this equation, because the optimal control is designed under the assumption that all coefficients a_{mk}^i are zero. We should also point out that matrix B_m does not depend on solar generation states, and therefore has no superscript associated with it.

Since this paper focuses on power system resiliency, our main objective in the following will be to optimize battery storage while satisfying the load demand when the MG clusters are in an islanded mode. Such an optimization requires a cost function that reflects the mismatch between the demand and the power delivered. This function will also have to take into account random variations in solar generation, which are due to changes in

cloud coverage. In order to meet these criteria, it will be necessary to introduce a change of variables [23], in which case the subsystem model becomes

$$\dot{\tilde{x}}_m(t) = A^i_m \tilde{x}_m(t) + B_m u_m(t), \qquad i = 1, 2, 3 \tag{27}$$

where

$$\tilde{x}_m(t) = \bar{x}_m(t) + \left(A^i_m\right)^{-1} \bar{P}^i_m \tag{28}$$

and

$$\bar{x}_m(t) = x_m(t) - x^i_{0m} \tag{29}$$

In expression (29), x^i_{0m} represents the desired energy setpoints for the battery and the load (which are mode dependent in general). Set point changes are designed to address two types of variations in the system: the discrepancy between the load demand during the day and at night, and fluctuations in power generation due to different cloud coverages. The vector $\bar{P}^i_m$ that appears in (28) is related to P^i as

$$\bar{P}^i_m = P^i_m + A^i_m x^i_{0m} \tag{30}$$

For the infinite horizon problem with performance measure

$$J = \overline{\lim_{t_f \to \infty}} \frac{1}{t_f} E \left\{ \int_{t_0}^{t_f} \left(\left(\tilde{x}_m(t) - \tilde{x}^i_{0m} \right)^T Q^i_m \left(\tilde{x}_m(t) - \tilde{x}^i_{0m} \right) + u_m^T(t) R^i_m u_m(t) \right) dt \right\} \tag{31}$$

(where $\tilde{x}^i_{0m} = \left(A^i_m\right)^{-1} \bar{P}^i_m$), the optimal discharge and charging patterns of the batteries is obtained by minimizing function J. This ensures that the error between the generation and the demand is as small as possible. The resulting optimal regulator is given as a time-varying feedback law

$$u^*_m(t) = -\left(R^i_m\right)^{-1} B^T_m K_{m\infty}^{\ i} \left(\bar{x}_m(t) + \eta^i_m(t) \right) \quad \text{for} \quad r(t) = i \tag{32}$$

It is important to emphasize once again that this gain matrix is independent of coefficients a^i_{mk}, since it is designed to optimize *decoupled* microgrids. As a result, the corresponding decentralized control laws can be computed offline for any given level of cloud coverage.

4. Suboptimality and Energy Exchanges

Since the optimal control law described in the previous section is designed to minimize cost function $J(t_0, x_0)$ when all subsystems are decoupled, we now need to consider what happens when the microgrids are allowed to exchange energy. In that case, coefficients a^i_{mk} will assume nonzero values, and the system will become *suboptimal*. If we denote the minimal value of the cost function in the disconnected mode by $J^o(t_0, x_0)$, this means that $J^c(t_0, x_0)$ (which corresponds to the case when subsystems are connected) will necessarily be larger. The following definition provided in [24] allows us to compare these two scenarios and evaluate the degree of suboptimality in the system.

Definition 1. Let $J^o(t_0, x_0)$ denote the optimal value of the cost function in the disconnected mode, and let $J^c_k(t_0, x_0)$ be the value that corresponds to the interconnection pattern k. The system is said to be *suboptimal with index ε* if

$$J^c_k(t_0, x_0) \le (1 + \varepsilon) J^o(t_0, x_0) \qquad \forall x_0 \in \mathbb{R}^n \tag{33}$$

Since suboptimality is a result of the interactions between the subsystems, index ε will obviously depend on their magnitude. Conditions that ensure the existence of such an

index are provided in Theorem 1, which represents a straightforward application to the result provided in [24].

Theorem 1. *The system described by Equations* (14) *and* (15) *with* $u_m = K_m x_m$ *is suboptimal with index* ε *if:*

$$\sum_{m=1}^{n} \sum_{k=1}^{n} a_{mk} \leq \frac{1}{2} \left(\frac{\varepsilon}{1 + \varepsilon} \right) \frac{\min_{m} \lambda_{min}[W_m]}{\max_{m} \lambda_{max}[K_m]} \quad \varepsilon > 0 \quad (34)$$

where λ_{min}, λ_{max} *are the minimal and maximal eigenvalues of the respective matrices, and*

$$W_m = K_m B_m R_m^{-1} B_m^T K_m + Q_m \quad (35)$$

In (35), K_m denotes the optimal gain matrix for subsystem m, while Q_m and R_m represent weighting matrices. Since K_m is calculated based on the choice of Q_m and R_m, these two matrices can be viewed as tuning parameters that allow the system to meet certain additional constraints. In the case of microgrids, the relevant constraints are defined by the upper and lower limits on battery storage levels, and the requirement that the load demand must be met in each subsystem.

In order to apply this result to jump linear systems, we need to modify Theorem 1 in the following way.

Theorem 2. *The system described by Equations* (14) *and* (15) *with* $u_m = K_m^i x_m$ *is suboptimal with index* ε_i *if*

$$\sum_{m=1}^{n} \sum_{k=1}^{n} a_{mk}^i \leq \frac{1}{2} \left(\frac{\varepsilon_i}{1 + \varepsilon_i} \right) \frac{\min_{m} \lambda_{min}[W_m^i]}{\max_{m} \lambda_{Max}[K_m^i]} \quad \varepsilon_i > 0 \quad (36)$$

where λ_{min}, λ_{max} *are the minimal and maximal eigenvalues of the respective matrices for each state* i *of the Markov chain, and* W_m^i *is given as*

$$W_m^i = K_m^i B_m^i (R_m^i)^{-1} (B_m^i)^T K_m^i + Q_m^i \quad (37)$$

As in the case of Theorem 1, the proof follows directly from the results provided in [24]. What makes this result particularly useful is the fact that it provides a simple upper bound for coefficients a_{mk}^i. These coefficients need to be adjusted every time one of the microgrids requests additional energy, so it is important to determine an appropriate exchange pattern quickly. We can do so because matrices K_m^i and W_m^i are computed *ahead of time* for each level of cloud coverage. This allows us to treat the right-hand side of inequality (38) as a known function of ε at the point when we need to choose new values for coefficients a_{mk}^i.

Remark 1. *It is important to recognize that the results described in this section remain valid regardless of how the cost function is chosen. It is therefore possible to adapt the proposed procedure to other types of constraints (such as those related to energy production or economic impact, for example). We intend to address this possibility in our future work.*

5. Simulation Results

In this section, we provide simulation results that were obtained using cloud coverage data from San Jose International airport [28], load data from NREL [27], and the Santa Clara University feeder. To keep the analysis as simple as possible, we considered a cluster of three microgrids, which can operate in the connected or disconnected mode, and can have different types of solar panels and battery storages. We assumed that one of the microgrids represents a university, and that the other two correspond to commercial MGs. Theorem 2 and the exchange protocol described in Section 2.3 were used to calculate the maximal amount of energy that can be transferred given a desired level of suboptimality.

For simulation purposes, we assumed that the battery storage and PV array of MG 3 are large enough to satisfy its own needs, and that the excess energy is shared with MGs 1 and 2. To better illustrate the potential benefits of the proposed approach, we additionally assumed that the battery storage and PV arrays for these two MGs do not produce enough energy to meet the demand at all times. Data from [28] were used to generate random cloud coverage patterns by Monte Carlo simulations, which determined the overall amount of solar generation at any given point in time.

Following the discussion in Section 1, we divided cloud coverage levels into three categories (which is representative of the weather pattern in northern California). Figure 2 provides the step-by-step procedure used to design the optimal regulator and calculate coefficients a_{mk}^i.
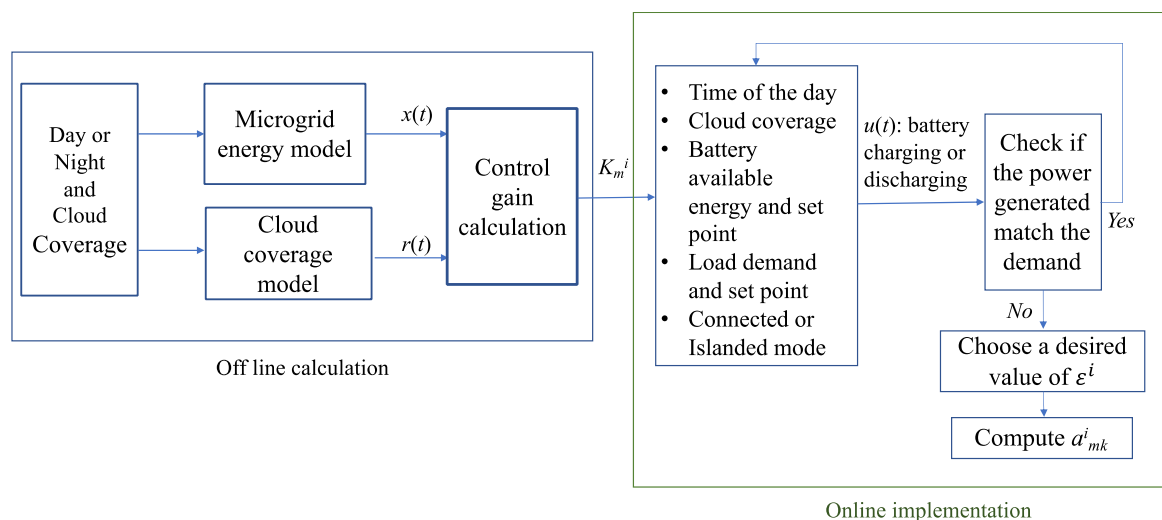
Figure 2. Procedure for calculating the optimal regulator gain and coefficients a_{mk}^i.

The results that we obtained are shown in Figures 3 and 4 (they cover a period of 5 business days). Since commercial load behavior is relatively predictable, we were able to use the load profile as a collection of setpoints instead of treating it as an input or a disturbance. In that respect, our approach differs from most other methods described in the literature. We should also note that due to the low or zero inertia related to batteries and solar energy, small imbalances between the supply and demand can be handled by batteries and PV arrays (or additional DC sources).

Figure 3 shows the simulation results for the three microgrids when they are in the *disconnected* mode. It is readily observed that all three batteries discharge to their lower limit at night, and that batteries in MGs 1 and 2 are unable to fully charge even when the weather is sunny (since their PV arrays are not sufficiently large). We should also point out that the load demands in MGs 1 and 2 (which are marked in blue in the bottom figure) are *not* met during peak hours.

The graphs in Figure 4 correspond to the situation where the three MGs are interconnected and can specify their needs through a communication network. When the demand in MG 3 is met and its battery is sufficiently full, energy is transferred to MGs 1 and 2. During these intervals, batteries 1 and 2 are able to charge.

To highlight the potential advantages of this approach, we considered a scenario where MGs 1 and 2 were able to fully satisfy their internal demand using the energy provided by MG 3. If this were not the case, MGs 1 and 2 could always connect to the utility grid and request the additional power that they need [26] (or possibly use a secondary source of generation). It is important to recognize, however, that the proposed scheme is helpful in such cases as well, because it reduces the amount of additional energy that is required. To evaluate the impact of energy exchanges in the latter scenario, we computed the integral of

the mismatch between the demand and supply over a five-day period. We found that the total error was reduced by about 8 MW, which is significant.
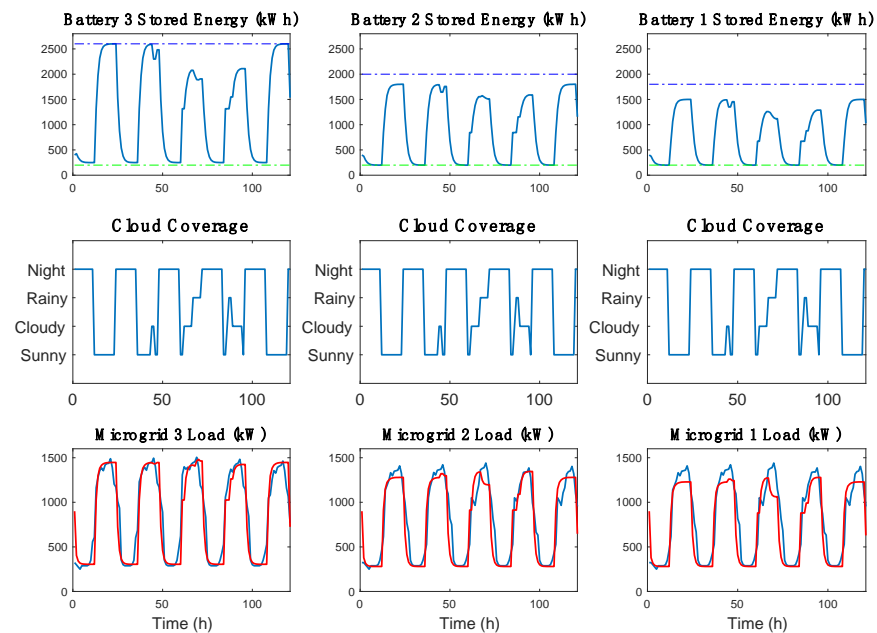
Figure 3. Simulation results when the microgrids are *disconnected*: battery energy variation (top figure), cloud coverage (middle figure), commercial load (blue) and load power usage (red) (bottom figure). The upper and lower dashed lines represent the minimum and maximum battery energy storage, respectively.
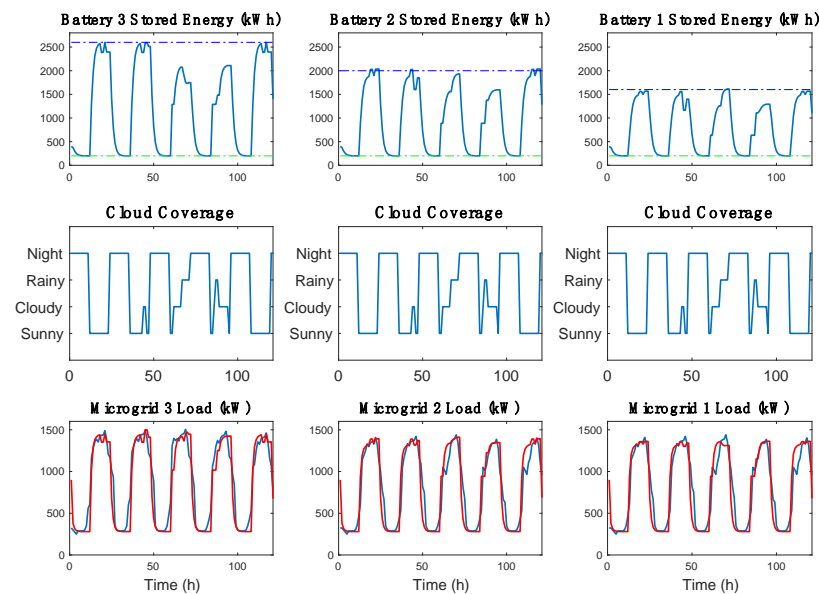
Figure 4. Simulation results when MGs 1–3 are *interconnected*: battery energy variation (top figure), cloud coverage (middle figure), commercial load (blue) and load power usage (red) (bottom figure).

6. Conclusions

In this paper, an optimal distributed stochastic control strategy was proposed for the energy management of MG clusters. A power balance model was developed that takes into account not only the randomness of solar generation, but also the exchange of power between MGs. The ε suboptimality index was used to compute the maximal amount of

energy that any MG can deliver or absorb for a given choice of ε. Simulation results using real data were provided for a cluster with three MGs.

The proposed approach was found to have the following advantages:

(1) Although it incorporates random variations in solar generation into the controller gains, it does not require an iterative algorithm to calculate the gain matrix. Because of that (and because all of the computations can be carried out offline), this method is suitable for real-time implementation.

(2) It allows the user to determine upper limits for the power exchange, based on the controller design. These limits were shown to be independent of the way in which the MGs are connected.

(3) The resulting decentralized control scheme guarantees stability for all possible interconnection patterns (as shown in Section 2.2).

(4) All the main features of this method can be easily adapted to networked MGs, since there is no restriction on how large n can be.

In our future work, we will consider possibilities for further improvement (such as incorporating the demand response into the model and considering different types of cost functions). We will also relax the assumption that the microgrids are physically close to each other, and that their loads have a known profile.

Author Contributions: Individual contributions are as follow: Conceptualization, M.K. and A.Z.; methodology, M.K. and A.Z.; simulation, M.K.; validation, M.K.; formal analysis, M.K. and A.Z.; investigation, M.K. and A.Z.; writing—original draft preparation, M.K.; writing—review and editing, M.K. and A.Z.; visualization, M.K. and A.Z. All authors have read and agreed to the published version of the manuscript.

Institutional Review Board Statement: Not applicable.

Informed Consent Statement: Not applicable.

Data Availability Statement: Publicly available datasets were analyzed in this study. This data can be found here: Commercial Load Modeling—System Advisor Model (SAM), National Renewable Energy Laboratory (NREL), sam.nrel.gov. Meteorological Aviation Routine Weather Reports (METAR/SPECI), San Jose International Airport (SJC), www.noaa.gov (accessed on 7 July 2021).

Conflicts of Interest: The authors declare no conflict of interest.

Nomenclature

Indices:

i, j	Indices for Markov chain states
m, k	Indices for microgrids
n	Maximum number of microgrids
q	Number of microgrids absorbing power

Parameters:

π_{ij}	Non-negative transition rate from i to j ($i \neq j$)
p_{ij}	Probability of transitioning from state i to state j
E_{Bmin}	Battery minimum energy limit (kWh)
E_{Bmax}	Battery maximum energy limit (kWh)
α_m	Fraction of solar power delivered to the load m
γ_m	Rate of self-charge for battery m (1/hour)
s_{ij}	Change in the operating points due to jumps from mode i to mode j
a_{km}	Fraction of power transferred from MG m to MG k

Matrices and Vectors:

$x(t)$	System state
x_0^i	Desired set point in mode i
$u(t)$	Control action,
$y(t)$	System output,
Π	Transition rate matrix
P	Probability matrix
$\eta^i(t)$	Bias vector for mode i
A^i	State matrix for mode i
B	Input matrix
C	Output matrix
P^i	Power delivered by the solar panels for mode i
Q^i	State weighting symmetric matrix for mode i
R^i	Input weighting symmetric matrix for mode i
K_∞^i	Riccati gain matrix for mode i at steady state

Variables:

$E_B^{(m)}(t)$	Energy stored in battery m (kWh)
$E_{ex}^{(m)}(t)$	Energy that MG m exchange with other MGs
$P_L^{(m)}(t)$	Power required by the load in MG m (kW)
$P_B^{dis(m)}(t)$	Power generated by the battery in MG m (kW)
$P_{Solar}^{(m)}(t)$	Power generated by the PV array in MG m (kW)
$P_{ex}^{(m)}(t)$	Power that MG m exchange with other MGs (kW)
$P(t)$	Power delivered by the solar panels (kW)
$r(t)$	Cloud coverage mode

References

1. Olivares, D.E.; Mehrizi-Sani, A.; Etemadi, A.H.; Cañizares, C.A.; Iravani, R.; Kazerani, M.; Hajimiragha, A.H.; Gomis-Bellmunt, O.; Saeedifard, M.; Palma-Behnke, R.; et al. Trends in microgrid control. *IEEE Trans. Smart Grid* **2014**, *5*, 1905–1919. [CrossRef]
2. Meng, L.; Shafiee, Q.; Trecate, G.F.; Karimi, H.; Fulwani, D.; Lu, X.; Guerrero, J.M. Review on control of DC microgrids and multiple microgrid clusters. *IEEE J. Emerg. Sel. Top. Power Electron.* **2017**, *5*, 928–948. [CrossRef]
3. Zou, H.; Mao, S.; Wang, Y.; Zhang, F.; Chen, X.; Cheng, L. A survey of energy management in interconnected multi-microgrids. *IEEE Access* **2019**, *7*, 72158–72169. [CrossRef]
4. Che, L.; Shahidehpour, M.; Alabdulwahab, A.; Al-Turki, Y. Hierarchical coordination of a community microgrid with AC and DC microgrids. *IEEE Trans. Smart Grid* **2015**, *6*, 3042–3051. [CrossRef]
5. Moayedi, S.; Davoudi, A. Distributed tertiary control of DC microgrid clusters. *IEEE Trans. Power Electron.* **2016**, *31*, 1717–1733. [CrossRef]
6. Shafiee, Q.; Dragičević, T.; Vasquez, J.C.; Guerrero, J.M. Hierarchical control for multiple DC-microgrids clusters. *IEEE Trans. Energy Convers.* **2014**, *29*, 922–933. [CrossRef]
7. Zhang, Y.; Xie, L.; Ding, Q. Interactive control of coupled microgrids for guaranteed system-wide small signal stability. *IEEE Trans. Smart Grid* **2016**, *7*, 1088–1096. [CrossRef]
8. Li, Y.; Dong, P.; Liu, M.; Yang, G.K. A distributed coordination control based on finite-time consensus algorithm for a cluster of DC microgrids. *IEEE Trans. Power Syst.* **2019**, *34*, 2205–2215. [CrossRef]
9. Dou, C.; Li, Y.; Yue, D.; Zhang, Z.; Zhang, B. Distributed cooperative control method based on network topology optimisation in microgrid cluster. *IET Renew. Power Gener.* **2020**, *14*, 939–947. [CrossRef]
10. Zaery, M.; Wang, P.; Wang, W.; Xu, D. Distributed global economical load sharing for a cluster of DC microgrids. *IEEE Trans. Power Syst.* **2020**, *35*, 3410–3420. [CrossRef]
11. Espina, E.; Llanos, J.; Burgos-Mellado, C.; Cárdenas-Dobson, R.; Martínez-Gómez, M.; Sáez, D. Distributed Control Strategies for Microgrids: An Overview. *IEEE Access* **2020**, *8*, 193412–193448. [CrossRef]
12. Han, Y.; Zhang, K.; Li, H.; Coelho, E.A.A.; Guerrero, J.M. MAS-based distributed coordinated control and optimization in microgrid and microgrid clusters: A comprehensive overview. *IEEE Trans. Power Electron.* **2018**, *33*, 6488–6508. [CrossRef]
13. Thieblemont, H.; Haghighat, F.; Ooka, R.; Moreau, A. Predictive control strategies based on weather forecast in buildings with energy storage system: A review of the state-of-the art. *Energy Build.* **2017**, *153*, 485–500. [CrossRef]
14. Kou, P.; Liang, D.; Gao, L. Distributed EMPC of multiple microgrids for coordinated stochastic energy management. *Appl. Energy* **2017**, *185*, 939–952. [CrossRef]
15. Xiao, F.; Ai, Q. New modeling framework considering economy, uncertainty, and security for estimating the dynamic interchange capability of multi-microgrids. *Electric Power Syst. Res.* **2017**, *152*, 237–248. [CrossRef]

16. Bazmohammadi, N.; Tahsiri, A.; Anvari-Moghaddam, A.; Guerrero, J.M. Optimal operation management of a regional network of microgrids based on chance-constrained model predictive control. *IET Gener. Trans. Distrib.* **2018**, *12*, 3772–3779. [CrossRef]
17. Lyu, Z.; Yang, X.; Zhang, Y.; Zhao, J. Bi-level optimal strategy of islanded multi-microgrid systems based on optimal power flow and consensus algorithm. *Energies* **2020**, *13*, 1537. [CrossRef]
18. Bazmohammadi, N.; Anvari-Moghaddam, A.; Tahsiri, A.; Madary, A.; Vasquez, J.C.; Guerrero, J.M. Stochastic predictive energy management of multi-microgrid systems. *Appl. Sci.* **2020**, *10*, 4833. [CrossRef]
19. Lan, Y.; Guan, X.; Wu, J. Online decentralized and cooperative dispatch for multi-microgrids. *IEEE Trans. Autom. Sci. Eng.* **2020**, *17*, 450–462. [CrossRef]
20. Chen, Z.; Yu, X.; Xu, W.; Wen, G. Modeling and control of islanded DC microgrid clusters with hierarchical event-triggered consensus algorithm. *IEEE Trans. Circuits Syst. I Regul. Pap.* **2021**, *68*, 376–386. [CrossRef]
21. Xu, Q.; Xu, Y.; Xu, Z.; Xie, L.; Blaabjerg, F. A hierarchically coordinated operation and control scheme for DC microgrid clusters under uncertainty. *IEEE Trans. Sustain. Energy* **2021**, *12*, 273–283. [CrossRef]
22. Lai, J.; Lu, X.; Wang, F. Bilevel information-aware distributed resilient control for heterogeneous microgrid clusters. *IEEE Trans. Ind. Appl.* **2021**, *57*, 2014–2022. [CrossRef]
23. Bullich-Massague, E.; Diaz-Gonzalez, F.; Aragues-Peñalba, M.; Girbau-Llistuella, F.; Olivella-Rosell, P.; Sumper, A. Microgrid clustering architectures. *Appl. Energy* **2018**, *212*, 340–361. [CrossRef]
24. Siljak, D.D. *Large Scale Dynamic Systems*; North Holland: New York, NY, USA, 1978.
25. Mariton, M. Control optimization. In *Jump Linear Systems in Automatic Control*; Marcel Dekker Inc.: New York, NY, USA, 1990; pp. 55–90.
26. Khanbaghi, M.; Zecevic, A. Jump linear quadratic control for microgrids with commercial load. *Energies* **2020**, *13*, 4997. [CrossRef]
27. Commercial Load Modeling—System Advisor Model (SAM), National Renewable Energy Laboratory (NREL). Available online: https://sam.nrel.gov/ (accessed on 20 July 2021).
28. Meteorological Aviation Routine Weather Reports (METAR/SPECI), San Jose International Airport (SJC). Available online: www.noaa.gov (accessed on 7 July 2021).
29. Levron, Y.; Guerrero, J.M.; Beck, Y. Optimal power flow in microgrids with energy storage. *IEEE Trans. Power Syst.* **2013**, *28*, 3226–3234. [CrossRef]
30. Zečević, A.; Khanbaghi, M. A Parallelizable algorithm for stabilizing large sparse linear systems with uncertain interconnections. *IEEE Access* **2022**, *10*, 35888–35899. [CrossRef]
31. Sworder, D.; Rogers, R. An LQ-solution to a control problem associated with a solar thermal central receiver. *IEEE Trans. Autom. Control* **1983**, *28*, 971–978. [CrossRef]
32. Ji, Y.; Chizeck, H.J. Controllability, stabilizability, and continuous-time Markovian jump linear quadratic control. *IEEE Trans. Autom. Control* **1990**, *35*, 777–788. [CrossRef]
33. Abou-Kandil, H.; Freiling, G.; Jank, G. Solution and asymptotic behavior of coupled Riccati equations in jump linear systems. *IEEE Trans. Autom. Control* **1994**, *39*, 1631–1636. [CrossRef]
34. Khanbaghi, M.; Malhamé, R.; Perrier, M. Optimal white water and broke recirculation policies in paper mills via jump linear quadratic control. *IEEE Trans. Control Syst. Technol.* **2002**, *10*, 578–588. [CrossRef]